한국압력기기공학회 논문집
제15권 제1호 2019년 6월 pp. 8-17

ISSN 1738-8333
http://dx.doi.org/10.20466/KPVP.2019.15.1.008

<연구논문>

Assessment of Equivalent Elastic Modulus of Perforated Spherical Plates

Collins JUMA† and Ihn NAMGUNG*

(Received 26 November 2018, Revised 18 June 2019, Accepted 18 June 2019)

ABSTRACT

Perforated plates are used for the steam generator tube-sheet and the Reactor Vessel Closure Head in the Nuclear Power Plant. The ASME code, Section III Appendix A-8000, addresses the analysis of perforated plates, however, this analysis is only limited to the flat plate with a triangular perforation pattern. Based on the concept of the effective elastic constants, simulation of flat and spherical perforated plates and their equivalent solid plates were carried out using Finite Element Analysis (FEA). The isotropic material properties of the perforated plate were replaced with anisotropic material properties of the equivalent solid plate and subjected to the same loading conditions. The generated curves of effective elastic constants vs ligament efficiency for the flat perforated plate were in agreement with the design curve provided by ASME code. With this result, a plate with spherical curvature having perforations can be conveniently analyzed with equivalent elastic modulus and equivalent Poisson's ratio.

Key Words : Perforated Plate, ASME code, Effective Elastic Constants, Isotropic Materials Properties, Anisotropic Material Properties, Ligament Efficiencies.

Nomenclature

η = Ligament efficiency
h = Nominal with of ligament
p = Distance between the centers of the holes (pitch)
d = Diameter of hole (=2R)
E^* = Effective Young's Modulus in plane stress condition
v^* = Effective Poisson's ratio in plane stress condition
G^* = Effective Shear Modulus in plane stress condition
v_0^* = Value of v^* when $v = 0.3$
$\overline{\overline{E}}^*$ = Effective Young's Modulus in plane strain condition
$\overline{\overline{v}}^*$ = Effective Poisson's ratio in plane strain condition.
$\overline{\overline{G}}^*$ = Effective Shear Modulus in plane strain condition.
$\overline{E}^*$ = Effective Young's Modulus in general plane strain condition.
$\overline{v}^*$ = Effective Poisson's ratio in general plane strain condition.
$\delta_{perforated\ plate}$ = Summation of deflection at finite point of perforated plate
$\delta_{=alent\ solid\ plate}$ = Summation of deflection at finite point of solid plate
$f(E',\ v')$ = Object functional symbolizing deference between solid plate and perforated plate deformation
δ_{Total} = Summation of difference in deformation of solid and perforated plate
$u_1 \cdots u_n$ = Deformation of solid plate at finite location $1 \cdots n$
$u_1' \cdots u_n'$ = Deformation of perforated plate at finite location $1 \cdots n$

† 1st Author, KEPCO International Nuclear Graduate School.
E-mail : inamgung@kings.ac.kr
Tel: (052)-712-7314
* Corresponding Author, KEPCO International Nuclear Graduate School

Introduction

In the nuclear industry, thick perforated plates are used for the steam generator tube-sheet and the Reactor Vessel Closure Head. Design and structural analysis of the perforated plate is based on the concept of the equivalent solid plate. The functional requirement of the steam generator tube-sheet and Reactor Closure Head is to provide support to the tubes and the nozzles, respectively.

The ASME Section III Appendix A-8000[1] provides a procedure for analysis of the perforated plate based on the equivalent solid plate concept. A solid plate with modified elastic constant values and geometrically similar to the perforated plate is used to analyze a perforated plate. This analysis method is applicable to the flat perforated plate subjected to direct loadings or loadings resulting from structural interaction with adjacent members provided the perforated plate:

i. Have circular holes in an array of equilateral triangles.
ii. A minimum number of holes is 19.
iii. Have a Ligament efficiency greater than 5% ($\eta \geq 0.05$).

Fig. 1 next page shows the ASME design curve showing the relationship between effective elastic constants and the equivalent material properties. Although ASME Section III Appendix A-8000 provides the procedure for determining the effective elastic constant, it is only applicable to a flat perforated plate and limited literature is available on the analysis of the spherical perforated plate. Extensive research has been carried out on the method of determining the equivalent material properties of a perforated plate based on the equivalent solid plate concept.[2],[3]

Horvay[2] and Malkin[3] developed numerical methods based on analyzing the stress and displacements in perforated structures that were geometric approximations of the actual perforated plate with circular holes in a doubly-periodic array. However, the solution obtained by these methods was limited to low ligament efficiencies.

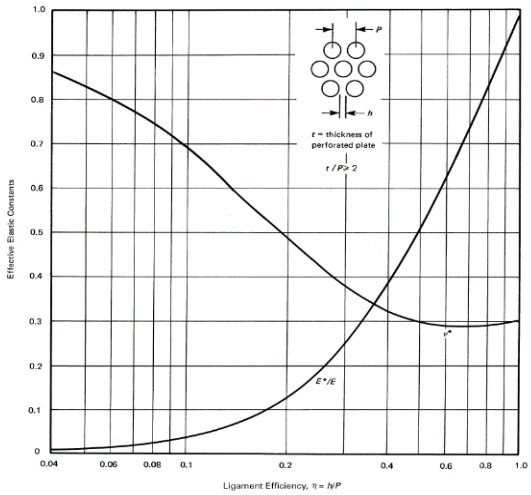

Fig. 1 Equivalent material properties[1]

Slot and O'Donnell[4] determined the effective elastic constants for a range of ligament efficiencies and Poisson's ratio. This was based on the concept that the deformation of the perforated plate is similar to that of the equivalent solid plate subjected to similar loading conditions.

Bailey and Hicks[5] theoretically obtained the design curve for determining the equivalent material properties. However, nonlinear equivalent material properties were not considered.

Duncan and Upfold[6] adopted the equivalent solid plate concept to determine the effective elastic constant. The isotropic material properties of the perforated plate were replaced with orthotropic material properties of an equivalent solid plate subjected to the same loading conditions.

This paper uses a optimization technique to assess the effective elastic constants for a flat and spherical plate with a triangular perforation pattern using the FEA simulation. Verification and validation of the FEA methodology for the flat plate was done according to the design and analysis requirements provided by ASME Section III Appendix A-8000. The same concept was then extended to spherical perforated plate.

1.1 Scope and Objective

The objective of this paper is to extend the equivalent

material constant concept to the spherical perforated plate based on the ASME code. To carry out this objective the following will be covered:

i. Review of available documents and previous research works.
ii. Determining the Equivalent constants based on ASME codes and standards.
iii. Developing of the 3D models of the perforated plates and their equivalent solid plates.
iv. Structural analysis using FEM to determine the equivalent material constants.
v. Developing of the design curves from FEM results and compare with the design curve provided in ASME codes.

1.2 Equivalent material properties for the flat perforated plate

The effective elastic constants are determined in such a way that the gross deformation in the perforated plate and the equivalent solid plate are identical under similar loading and boundary conditions. Equivalent material constants are used to simulate the behaviour of the perforated plate as an equivalent solid plate and are obtained based on the ligament efficiency (η) as well as the ratio of nominal width of ligament to pitch (h/p) as shown in Fig. 2 below. The ligament efficiency (η) is defined by equation (1).

$$\eta = \frac{h}{p} = \frac{p-d}{p} \tag{1}$$

ASME code [1] gives equivalent elastic constants for a plane stress conditions. However, for a thick plate relative to the diameter of the perforation, generalized plane strain conditions are more realistic. Hence, the relationship between effective elastic constants for both plane stress and the generalized plane strain conditions was formulated [4].

Based on the theory of elasticity, stresses, strain, and displacement of a perforated plate under plane stress condition are defined by:

$$E^* = \frac{\sigma^*}{\varepsilon^*} \tag{2}$$

$$G^* = \frac{\tau^*}{\gamma^*} \tag{3}$$

$$\varepsilon_x = \partial_u / \partial_x = (\tau_x - v\sigma_y)/E \tag{4}$$

$$\varepsilon_y = \partial_v / \partial_y = (\sigma_y - v\sigma_x)/E \tag{5}$$

$$\gamma_{xy} = \partial_u / \partial_y + \partial_v / \partial_x = \tau_{xy}/G \tag{6}$$

Where (*) is the equivalent properties.

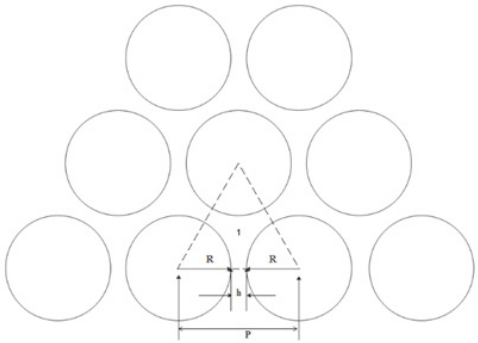

Fig. 2 Plane view of the triangular perforate plate.

The relationship between the plane stress constants and material constants can be expressed such that the Effective Young's modulus (E^*) is directly proportional to Young's modulus (E) of the perforated plate material while the effective Poisson's ratio (v^*) is linearly dependent on the Poisson's ratio (v) of the material[6] and this can be defined by:

$$E^* = EF(\eta) \tag{7}$$

$$v^* = G(\eta) + vF(\eta) \tag{8}$$

For a given value of ligament efficiency (η) where $F(\eta)$ and $G(\eta)$ are constants. The function $G(\eta)$ provides a value of $v^* = V_0^*$ for $v = 0$ which is an intercept value.

Substituting equations (7) in (8)

$$v^8 = v_0^* + \left(\frac{E^*}{E}\right) v \tag{9}$$

Effective elastic constants are obtained by superposition

of strain ($\varepsilon_z = 0$). For plane strain condition, ($\varepsilon_z = 0$)

$$E^* = \frac{E^*}{(1-v^2)} \tag{10}$$

$$v^* = v_0^* + \left(\frac{vE^*}{E(1-v)}\right) \tag{11}$$

$$G^* = \frac{E^*}{2(1+v^*)} \tag{12}$$

Therefore equivalent solid plate stress-strain relation under plane strain condition can be given by

$$\varepsilon_x^* = \sigma_x^*/\overline{\overline{E}}^* \; - \; \overline{\overline{v}}^* \; \sigma_y^*/\overline{\overline{E}}^* \tag{13}$$

$$\varepsilon_y^* = \sigma_y^*/\overline{\overline{E}}^* \; - \overline{\overline{v}}^* \sigma_x^*/\overline{\overline{E}}^* \tag{14}$$

$$\gamma_{xy}^* = \tau_{xy}^*/\overline{\overline{G}}^* \tag{15}$$

Given that $G^* = \overline{\overline{G}}^*$

For plane strain $\varepsilon_z = 0$

$$\varepsilon_z = \sigma_z/E - \frac{v(\sigma_x + \sigma_y)}{E} = 0 \tag{16}$$

Where

$$\sigma_z = (\sigma_x + \sigma_y) \tag{17}$$

Considering that the perforated plate is relatively thick in comparison with the pitch dimension, the equivalent elastic constants are determined based on the generalized plane strain condition.

$\varepsilon_z = uniform$ And σ_z vanishes in a general plane strain. Therefore the effective elastic constants are obtained by superposition of strain produced under plane strain condition and strains that results from annihilating the associated average surface traction $\sigma_z^{*(3)}$.

$$\varepsilon_x^* = v\sigma_z^*/E_z^* = v^2(\sigma_x^* + \sigma_y^*)/E_z^* \tag{18}$$

$$\varepsilon_y^* = v\sigma_z^*/E_z^* = v^2(\sigma_x^* + \sigma_y^*)/E_z^* \tag{19}$$

$$\gamma_{xy}^* = 0 \tag{20}$$

The effective Young's modulus for the triangular penetration in the thickness direction is obtained by multiplying E with the ratio of the net surface are of the perforated plate and the total area of plate

Triangular area: $\sqrt{3}/4p^2$

Triangular area with hole:

$$\sqrt{3}/4p^2\{1-\pi/2\sqrt{3}(1-n)^2\}$$

The ratio of

$$E_z^*/E = \left(1 - \frac{\pi(1-\eta)^2}{2\sqrt{3}}\right) \tag{21}$$

The effective Young's modulus and the Poisson's ratio are related to the plane stress by the following equations:

$$\overline{E}^* = \left[\frac{(1-v^2)}{E^*} + \frac{v^2}{E_z^*}\right]^{-1} \tag{22}$$

$$\overline{v}^* = E^* \times \left[\frac{(1-v^2)v_o^*}{E^*} + \frac{v(1+v)}{E} - \frac{v^2}{E_z^*}\right] \tag{23}$$

$$v^* = v_o^* + \left(\frac{E^*}{E}\right)v \tag{24}$$

Substituting V_O^* of equation (9) in (8)

$$\overline{v}^*\left(\frac{\overline{E}^*}{E}\right) = \left[v^3 + v^2\left(1 - \frac{E^*}{E_z^*}\right) + (1-v^2)v^*\frac{E}{E^*}\right] \tag{25}$$

2. Methodology

2.1 Modeling of perforated and equivalent solid plate

In this study, the equivalent material properties for a flat perforated plate was extended to the spherical perforated plate. Using FEA, the perforated plates, both Flat and Spherical, with triangular perforation patterns and their equivalent solid plates of uniform thickness 5mm were developed. The triangular perforations pattern on the plate was defined by circular

holes with a radius of 9.5mm normal to the plate surface with a pitch of 20 mm as shown in Fig. 3 for flat plate, Fig. 4 for circular plate with parallel holes and Fig. 6 for circular plate with concentric holes.

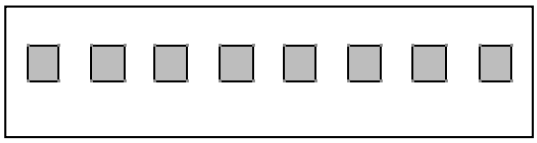

Fig. 3 Flat perforated plate

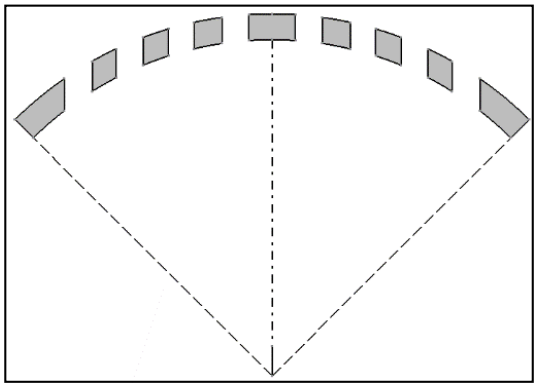

Fig. 4 Perforations parallel to the plate surface.

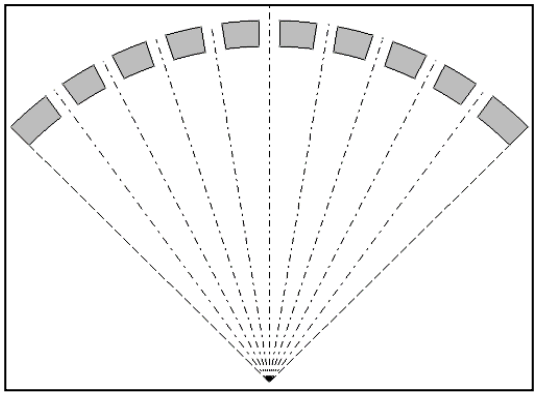

Fig. 5 Perforations normal to the plate surface.

Ligament efficiencies (η) for a given range of $0.05 \leq \eta \geq 1$[(1)] were computed.

2.2 Loading conditions and material definition.

A pressure of magnitude 2 MPa acting normal to the solid surface area of the perforated plate in the z-direction with different ligament efficiencies was made equal to that acting normal to the equivalent solid plate surface. This was to ensure both the perforated and the equivalent solid plate are subjected to the similar loading condition as shown in Fig. 6, Fig. 7, Fig.8, Fig.9, Fig.10 in the next page.

Perforated plate isotropic material properties were replaced with anisotropic properties of the equivalent solid plate. Engineering constants of the perforated plates were defined as $E = 200\,GPa$, $v = 0.3$ and, $G = 76.92\,GPa$.

2.3 Optimization

Since the perforated and equivalent solid plate are subjected to the same loading conditions, the overall deformation is the same [(3)].

$$\delta_{perforatedplate} = \delta_{Equivalent\ Solid\ Plate} \tag{26}$$

From the FEA simulation, deformation on different points equally spaced on both the perforated and equivalent solid plate was determined. Optimization for the deformation of the perforated and equivalent solid plate was carried out by varying the values of the equivalent material properties so that the summation of the difference of the absolute value for deformation convergence.

$$f(E',\ v') \equiv \delta_{Total} = 0 \tag{27}$$

$$\delta_{Total} = |u_1 - u_1'| + |u_2 - u_2'| + ..|u_{n+1} - u_{n+1}'| \tag{28}$$

Inevitably, considerable FEA simulation was involved for different values of ligament efficiencies for the flat and spherical perforated plate and their equivalent solid plates. This is summarized in Fig. 11 below. Because the optimization involves two independent variables, i.e. E and v, it produces two dimensional functional surface. After initial search is done, a proximal point near true optimal location can be obtained. A second round search around proximal point gives optimal value of E and v.

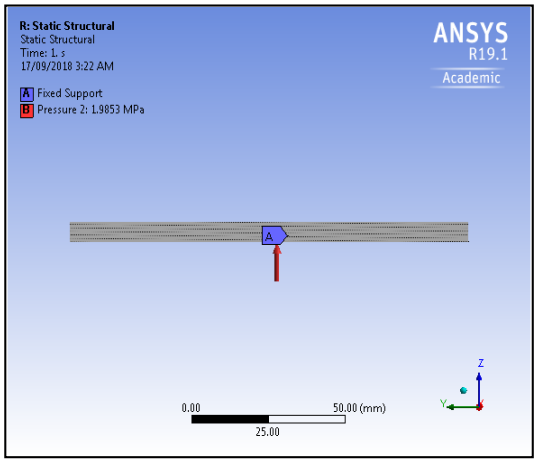

Fig. 6 Equivalent Flat Solid Plate loading and B.C.

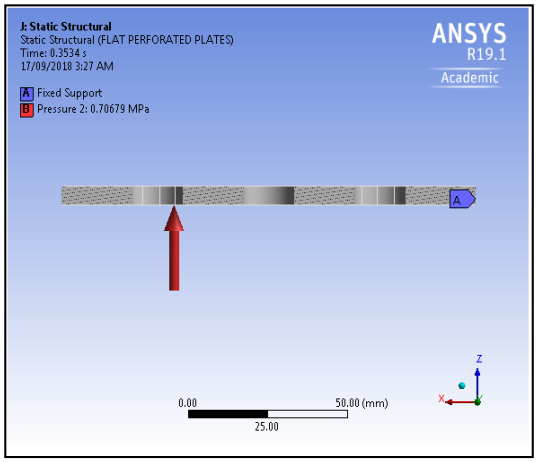

Fig. 7 Flat perforated plate loading and B.C.

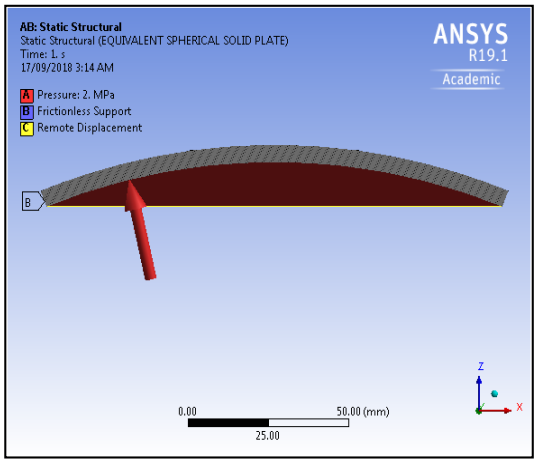

Fig. 8 Equivalent spherical solid plate loading and B.C.

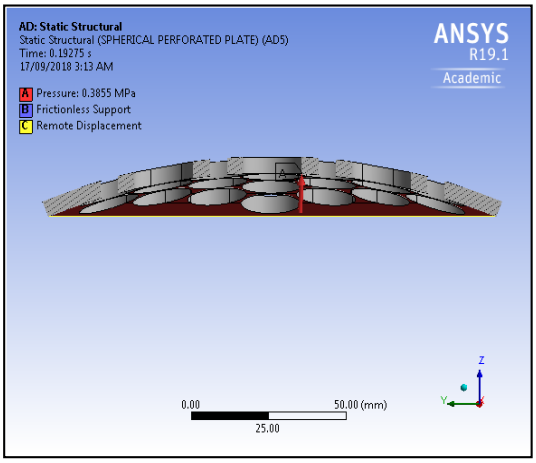

Fig. 9 Spherical perforated plate loading and B.C.

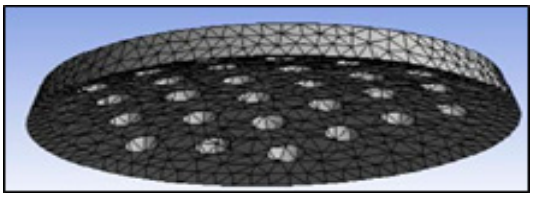

Fig. 10 An example of mesh plot with quadratic elements.

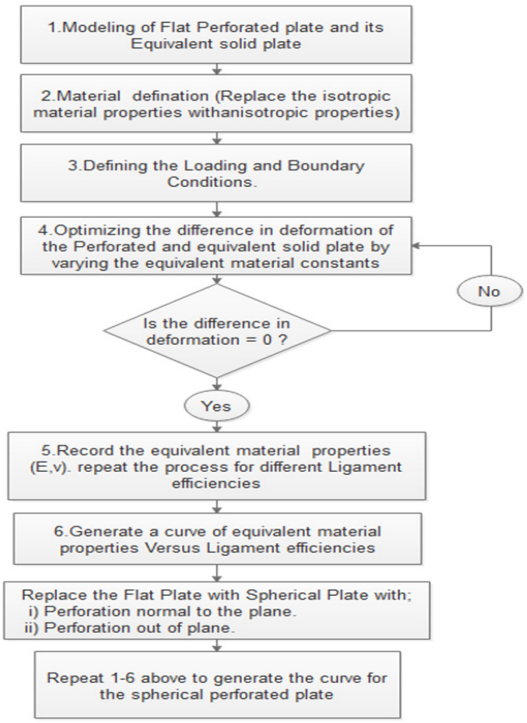

Fig. 11 Procedure to determine the equivalent material constants

3. Results

As mentioned earlier, the aim of this research is to extend the equivalent material concept to the spherical perforated plate. Flat and spherical plates with triangular perforation patterns normal to the surface were considered. Additionally, a spherical plate with perforation parallel to the surface was also considered.

3.1 Flat perforated plate

FEA analysis was first carried out to re-assess the ASME design curve for the flat perforated plate. The effective elastic constants obtained for different ligament efficiencies were tabulated as shown in Table 1 below. The curves of the equivalent material properties versus the ligament efficiencies were then generated as shown in Fig. 12 below.

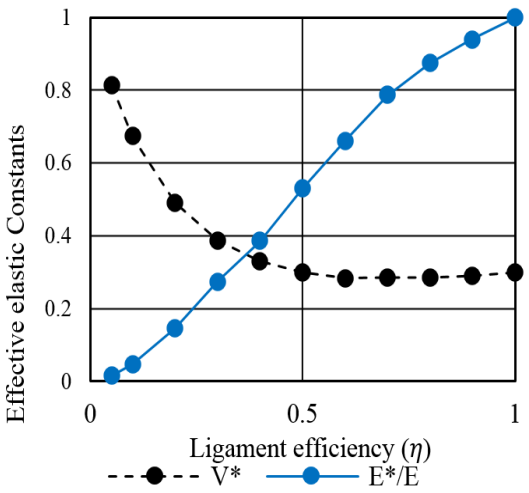

Fig. 12 Flat perforated plate equivalent material properties

To verify the FEA methodology used to determine the equivalent material properties for the flat plate, the curves were compared to the design curves provided in the ASME Section III Appendix A-8000. The curves are in good agreement with the design curve. Evidence for this is shown in Fig. 13 below.

Table 1 FEA results for equivalent material constants.

η	E^*/E	$v^*(v=0.3)$
0.05	0.015	0.815
0.1	0.048	0.673
0.2	0.145	0.490
0.3	0.275	0.388
0.4	0.385	0.330
0.5	0.53	0.299
0.6	0.66	0.283
0.7	0.785	0.286
0.8	0.875	0.284
0.9	0.94	0.290
1.0	1	0.30

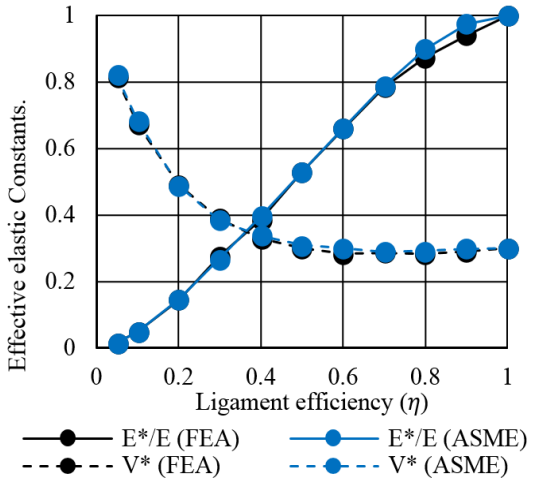

Fig. 13 Comparison of FEA result effective elastic constants and ASME design curves.

3.2 Spherical perforated plate

3.2.1 Case 1: Spherical plate with perforations parallel to the plane.

The FEA methodology and the concept of an equivalent elastic constant for a flat perforated plate were extended to the spherical perforated plate. FEA results for the equivalent elastic constants were tabulated as shown in Table 2 next page.

The curves of the equivalent material properties versus the ligament efficiencies were then generated as shown in Fig. 14 previous page.

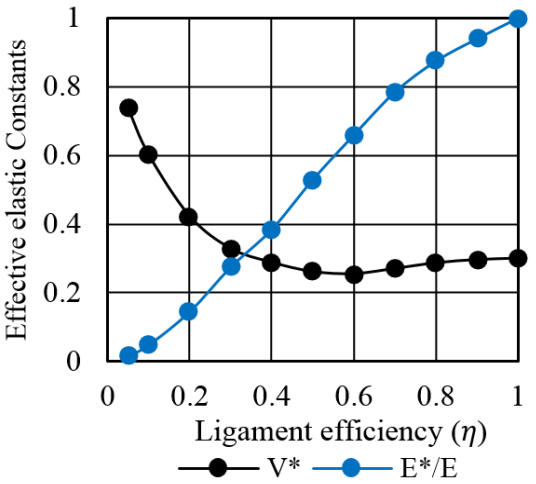

Fig. 14 Equivalent elastic constants for a spherical plate with perforation parallel to the plane.

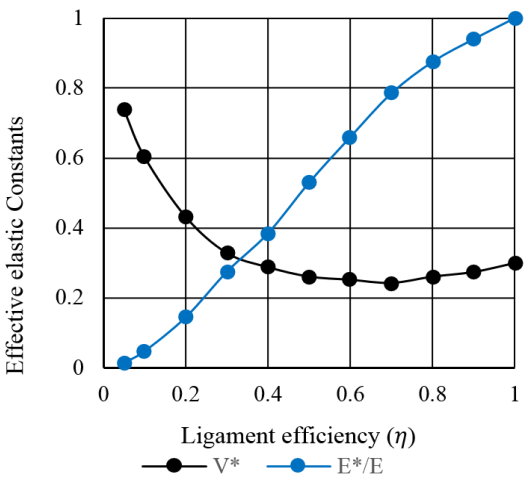

Fig. 15 Equivalent elastic constants for a spherical plate with perforation normal to the surface

Table 2 Equivalent elastic constants.

η	E^*/E	$v^*(v=0.3)$
0.05	0.015	0.738
0.1	0.048	0.603
0.2	0.145	0.423
0.3	0.275	0.329
0.4	0.385	0.288
0.5	0.53	0.261
0.6	0.66	0.255
0.7	0.785	0.270
0.8	0.875	0.287
0.9	0.94	0.296
1.0	1	0.30

Table 3 Equivalent elastic constants.

η	E^*/E	$v^*(v=0.3)$
0.05	0.015	0.738
0.1	0.048	0.603
0.2	0.145	0.432
0.3	0.275	0.329
0.4	0.385	0.288
0.5	0.53	0.261
0.6	0.66	0.252
0.7	0.785	0.243
0.8	0.875	0.261
0.9	0.94	0.274
1.0	1	0.30

3.2.2 Case 2: Spherical plate with perforations normal to the surface.

The results for the spherical plate with perforation out of the plane was tabulated as shown in Table 3 below.

The curves of the equivalent material properties versus the ligament efficiencies were then generated as shown in Fig. 15 below.

The curves of the equivalent material properties of the spherical perforated plate with perforation normal to the surface and parallel to the plane were compared as shown in Fig. 16 below.

The curves of the flat and spherical plates for both cases i.e. with perforation normal to the surface and parallel to the plane were compared as shown in Fig. 17 above.

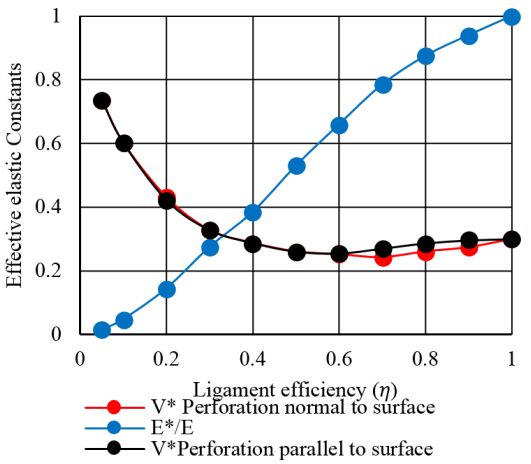

Fig. 16 Comparison of the equivalent material properties of the spherical plate with perforation normal to the surface and parallel to the plane.

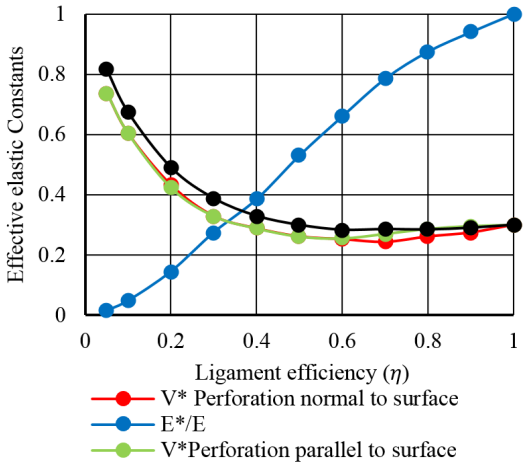

Fig. 17 Comparison of the equivalent material properties of the flat and spherical plate with perforation normal to the surface and parallel to the plane.

4. Discussion and Conclusion

ASME Section III Appendix A-8000, states the methodology for the design and analysis of perforated plates. However, the methodology is limited to the flat perforated plate. This study incorporated optimization technique in finding the equivalent material concept to the spherical perforated plate by FEA analysis.

Verification and validation ensure that the design and analysis of the perforated and equivalent solid plates were done as per requirements. FEA methodology developed to determine the equivalent material properties was validated by comparing the curves generated from the FEA results with the design curve provide in ASME codes. The curves are in good agreement as expected, but not precise due to the degree of mesh refinement of the plates. Hence, for more accurate results fine mesh is required in the vicinity of the perforations which in turn more time is required to carry out the analysis.

The trend of curves of the equivalent material properties versus the ligament efficiency for the spherical perforated plate is similar to that of the flat perforated plate although it is lower. This is due to the fact that the deformation of the spherical plate is less compared to a flat plate subjected to the same loading condition.

The equivalent material properties of the spherical plate with perforation normal to the surface and parallel to the plane are similar. This indicates that the orientation of the perforation does not have an effect on the equivalent material constants. Hence, the same design curve can be used for a spherical plate with perforation normal to the surface and parallel to the plane.

The results from the FEA analysis prove that the equivalent material properties can be used in the design and analysis of the spherical perforated plate with perforations normal to and out of the plane. However, some limitations are worth noting. Modeling of the perforated plates and construction of fine meshing is quite complex and analysis require more time. Additionally, to determine the equivalent material properties several optimizations have to carry out. Future work should, therefore, include an experimental analysis to verify the equivalent material properties for a spherical perforated plate.

Acknowledgment

This research was supported by KEPCO International Nuclear Graduate School (KINGS). The authors would like to express their appreciation towards KINGS.

References

(1) ASME BPVC Sec.III, 2010, “Rules for Construction of Nuclear Facility Component, Division 1, Appendix A-8000, Stresses in Perforated Flat Plates,” American Society of Mechanical Engineers, New York

(2) Horvay, G, 1925, “The plane stress problem of perforated plates,” *Journal of. Applied Mechanics, Transactions of. ASME*, Vol. 74, pp. 355-360

(3) Malkin, T., 1952, “Notes on a theoretical basis for the design of tube sheets of triangular layout,” *Journal of. Applied Mechanics, Transactions of. ASME*, Vol. 74, pp. 389-396

(4) Slot, T., and O'Donnell, W.J., 1971, "Effective elastic constants for thick perforated plates with square and triangular penetration pattern," *Journal of. Applied Mechanics, Transactions of. ASME*, Vol. 93, pp. 1081-1088

(5) Bailey, R. and Hicks, R., 1960, "Behaviour of perforated plates under plane stress," *Journal of. Applied Mechanics, Transactions of. ASME.,* Vol. 2, (2), pp. 143-161

(6) Duncan, J.P. and Upfold, R.W., 1963, "Equivalent elastic properties of perforated bars and plates," *Journal of. Mechanical Engineering and Science.,* Vol. 15, (1), pp. 53-65

(7) Meijers. P., 1969, "Plate with a Doubly-Periodic Pattern of Circular Holes Loaded in Plane Stress or in Bending," ASME Publication on First International Conference on Pressure Vessel Technology, Delft, the Netherlands